An investigation of flush off-takes for use in a cooled cooling air system

An Investigation of Flush Off-Takes for Use in a Cooled Cooling Air System

Praveen Elango* **and A. Duncan Walker†**

Department of Aeronautical and Automotive Engineering, Loughborough University, Loughborough, LE11 3TU.

ABSTRACT

The design and evaluation of off-takes has traditionally focused on increasing ram pressure recovery with little consideration given to flow uniformity. Preliminary studies on a proposed cooled cooling air system for a large aero gas turbine indicated that the off-take represented a weak point in the design with the non-uniformities it generated negatively affecting system performance. High levels of diffusion and a uniform flow are required to minimise loss and to maximise the effectiveness of the downstream heat exchanger. This paper presents a numerical and experimental parametric study of parallel wall flush off-takes with focus placed on the quality of the downstream flow and its uniformity. A realisable k-omega turbulence closure was employed with a standard wall function to examine the pressure recovery and uniformity of flush off-takes. The performance of the off-take was investigated with different inflow boundary layer thicknesses in conjunction with changes in various design parameters. The current investigation highlights that there exists a direct trade-off between the diffusion and uniformity that can be achieved by a flush off-take. Nevertheless, the work provides an improved understanding of how each performance parameters can be maximised with respect to uniformity and this knowledge is currently being applied to the development of an optimal off-take design.

NOMENCLATURE

A	-	Area
AIP	-	Agreed Interface Plane
AR	-	Area Ratio
AS	-	Aspect Ratio
B	-	Blockage
B.L	-	Boundary Layer
CS	-	Capture Stream Tube
d	-	Depth (Off-take Height)
h	-	Height
HP	-	High Pressure
i	-	Intake or Off-take
L	-	Length
LP	-	Low Pressure
$\dot{m}$	-	Mass Flow Rate
MFR	-	Mass Flow Ratio
P	-	Total Pressure
p	-	Static Pressure
RPR, η	-	Ram Pressure Recovery
SDUI	-	Standard Deviation Uniformity Index
U	-	Velocity
VR	-	Velocity Ratio
w	-	Width

Symbols

α	-	Ramp Angle
δ	-	99% Boundary Layer Thickness
θ	-	Duct or Off-take Angle
∞, o	-	Onset Free Stream

INTRODUCTION

Air traffic is expected to grow significantly over the coming decades and, unless new technologies are introduced, this will negatively impact the environment due to increased emissions of CO_2, NO_x, CO, Unburnt Hydrocarbons (UHC), and particulate matter. Stringent legislation is in place to control the environmental impact of aviation, against which aircraft and aero engines must be certified. As aero gas turbine designers strive for ever greater efficiencies (and reduced fuel burn) the trend has been for engine overall

* PhD Research Student, Email: P.elango@lboro.ac.uk

† Senior Lecturer in Applied Aerodynamics, Email: A.D.Walker@lboro.ac.uk

pressure ratios (OPR) to rise. Higher OPR allows greater thermal efficiencies and provides higher thrust for a given core size. However, this also means that cycle temperatures increase. In modern aero engines the compressor exit temperature is now higher than the turbine entry temperature in early engines. This is a particular problem as compressor exit air is routinely used to cool components in the combustion and turbine systems. Using higher temperature air for cooling will reduce the operational life of these critical parts or require unacceptably high cooling flows, which will negate the ultimate goal of a reduction in specific fuel consumption.

Additionally, the drive towards lean-burn combustion systems, in order to reduce NOx emissions, further complicates this. For example, to enable lean operation the availability of turbine cooling air will be reduced; current engines require as much as 20-30% of the compressor delivery air to be diverted for component cooling. In summary, the task of cooling the highly thermally loaded turbine (both nozzle guide vane and rotor) will become considerably more difficult. One suggested solution, illustrated in Figure 1, is for some of the compressor efflux to be diverted for additional cooling in a heat exchanger (HX) cooled by air from the engine's bypass duct.

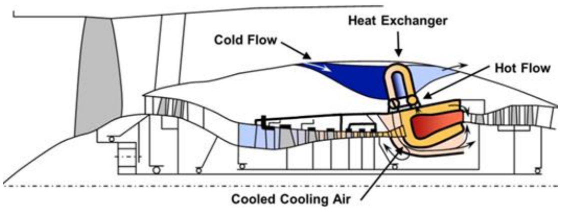

Figure 1: Schematic of a cooled cooling air system [1]

A cooled cooling air (CCA) system can be broken into three aerodynamic sub-systems each with their own set of requirements and challenges i.e (LP, HP and HX). The high pressure hot flow system has been studied by Walker et al. [2] but to date little attention has been given to the low pressure cold flow system. Preliminary numerical studies on an initial LP system indicated that the off-take was the weak point in the design. It was unable to deliver air of sufficient quality such that the flow could then tolerate the required levels of diffusion prior to the heat exchanger. Historically, the design of off-takes has focused on their pressure recovery and not the condition or uniformity of the flow delivered to the downstream components. Consequently the current work will focus more on this aspect in order to develop a flush off-take suitable for a CCA system.

PERFORMANCE PARAMETERS

In general, off-takes can be classified as flush (submerged) and scoop (pitot). For an off-take mounted in a bypass duct a flush design is preferred as it does not protrude into the bypass and generate excessive drag. They also have the advantage of being shorter and have higher flexibility in terms of location.

Off-take performance can be assessed by different methods such as the inlet pressure differential, total pressure ratio, total pressure loss or total pressure recovery [3]. However, the ram pressure recovery (RPR), or the ram ratio, is the most widely adopted method to assess performance. This is defined in Equation 1 as:

$$\eta, (RPR) = \frac{P_{AIP} - p_0}{P_0 - p_0} \quad (1)$$

Where 'AIP' is an agreed interface plane and '0' is the onset free stream. The performance of an off-take is always represented with reference to the operating mass flow (or similar flow parameters). The Mass Flow Ratio (MFR) is defined in Equation 2 as the ratio of mass flow at the AIP to the mass flow of the free stream with the same cross sectional area as that of the AIP. For an incompressible flow, the mass flow ratio term is simplified to Velocity Ratio (VR) which can be defined as the mean velocity at an AIP to the mean velocity at the free stream. It is more convenient to use VR as it is generally easy to measure during experiments.

$$\frac{\dot{m}_{AIP}}{\dot{m}_0} = \frac{\rho_{AIP}}{\rho_0}\frac{\overline{U}_{AIP}}{\overline{U}_0} = \frac{\overline{U}_{AIP}}{\overline{U}_0} \qquad (2)$$

Traditionally the design and evaluation of off-takes has primarily focused on increasing the ram pressure recovery while the uniformity of flow exiting an off-take has been given limited consideration. Any non-uniformity present in the flow exiting an off-take has the potential to negatively affect the performance of downstream components. In the current study the uniformity of the flow exiting the off-take was assessed based on the velocity field.

Figure 2 shows axial velocity contours plotted at an AIP (agreed interface plane) downstream of the off-take.

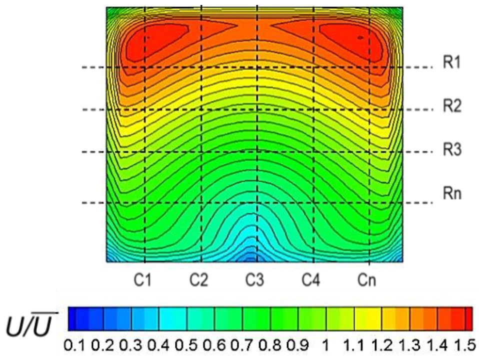

Figure 2: Example of an AIP with Index Planes

Bissinger and Breuer [4] give several commonly used parameters for expressing the non-uniformity or distortion:

DCθ	-	The critical angle low total pressure distortion coefficient
KDA	-	The radially weighted circumferential distortion parameter
IDCL	-	Inlet distortion circumferential coefficient
DI	-	Distortion index

These are relatively complex methods and mainly used for assessment of compressor performance or evaluation of distortion in circular ducts. In the current investigation the non-uniformity index has been evaluated by simply considering the standard deviation of the axial velocity. This is initially computed for the whole plane:

$$SDUI = \sqrt{\sum \frac{(U_x - \overline{U}_{axialplane})^2}{\mathrm{Total \cdot nodal \cdot points.at.AIP}}} \qquad (3)$$

However, Equation 3 does not represent whether the non-uniformity is predominantly along the horizontal or vertical direction. Hence the plane is divided into 'n' number of rows and columns. The nodal values in each row and column can then be combined and a mean horizontal or vertical standard deviation could be computed (equations 4 and 5). The horizontal non-uniformity ($SDUI_H$) and vertical non-uniformity ($SDUI_V$) can then be calculated separately by equations 6 and 7:

$$\sigma_{Cn} = \sqrt{\sum \frac{(U_{Cx} - \overline{U}_{Cx})^2}{n_{Cx}}} \qquad (4)$$

$$\sigma_{Rn} = \sqrt{\sum \frac{(U_{Rx} - \overline{U}_{Rx})^2}{n_{Rx}}} \qquad (5)$$

$$SDUI_H = \sqrt{\frac{\sum_{i=1}^{n} \sigma_{cn}^2}{n}} \qquad (6)$$

$$SDUI_V = \sqrt{\frac{\sum_{i=1}^{n} \sigma_{Rn}^2}{n}} \qquad (7)$$

Where:
U_{cx} is the axial velocity at a nodal point 'Cx'
$\overline{U}_{Cx}$ is the mean axial velocity at the plane 'C_n',
n_{cx} is the total nodal values at the plane 'C_n'
U_{Rx} is the axial velocity at a nodal point 'Rx'
$\overline{U}_{Rx}$ is the mean axial velocity at the plane 'Rn'
n_{Rx} is the total nodal values at the plane 'Rn'.

Lower SDUI values indicate an improved global uniformity along an AIP. The relative vertical or horizontal non-uniformity factor can be estimated by the difference of $SDUI_V$ or $SDUI_H$ with the SDUI respectively. The accuracy of the SDUI factor is increased by increasing the number of vertical and horizontal dividing planes ('n_{cx}' and 'n_{Rx}') taken along an AIP.

EXPERIMENTAL METHODOLOGY

To build a LP fan, bypass duct and off-take at engine scale would be an expensive approach for experimentation. In order to reduce the build cost, time of manufacturing and suit the available test facility the parallel wall flush off-take was scaled down to atmospheric lab conditions. An isothermal test rig was designed as depicted in Figure 3. Ambient air was fed to a large settling chamber via a main centrifugal fan. The air was then passed through a metered bell-mouth and filter screens in order to reduce any flow distortions. The total mass flow entering the rig was controlled by varying the fan speed and measured using the calibrated bell-mouth.

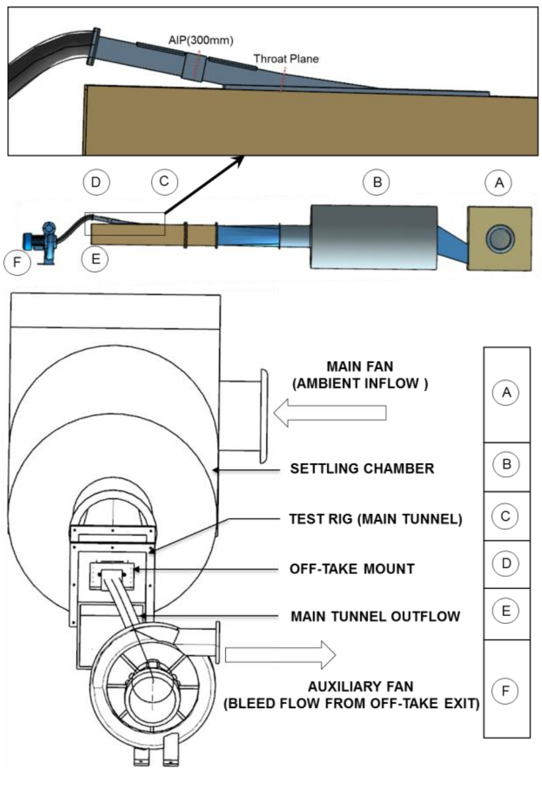

Figure 3: Experimental Set-Up

The test rig itself was a simple square tunnel of length 1500mm and of cross section 300mm x 300mm. A parallel wall flush off-take with a 7° ramp, a 10° duct angle, an aspect ratio of 1 and depth (d) of 50mm was mounted on one wall. The lip of the off-take was of radius 2mm. The off-take mass flow, and hence the velocity ratio, was controlled by an auxiliary fan placed downstream of the off-take. A traverse mechanism was installed to enable a miniature five-hole probe to be traversed at the inlet, the throat plane and an AIP at 300mm downstream of the off-take throat. All tests were performed at a Reynolds number of approximately 500,000 with an inlet velocity of 30m/s. The auxiliary fan was operated at different speeds to regulate the required flow through off-take at velocity ratios of 0.3, 0.5, 0.7 and 0.9 respectively.

CFD METHODOLOGY

Numerical studies were used to explore the design space and utilised the commercial CFD code ANSYS Fluent to model a generic flush off-take (Figure 4). The computational model comprised a bypass tunnel of length 600mm, cross-sectional width and height of 300mm. A hybrid structured mesh was employed and after a grid dependency study the final mesh had close to 2 million cells. A realizable k-omega turbulence closure was employed in conjunction with a standard wall function. Initial setup of the off-take inflow boundary layer was guided by the work reported by Devine et al. [5]. A naturally developed boundary layer profile of thickness δ/d=1.5 was used as an initial inflow condition.

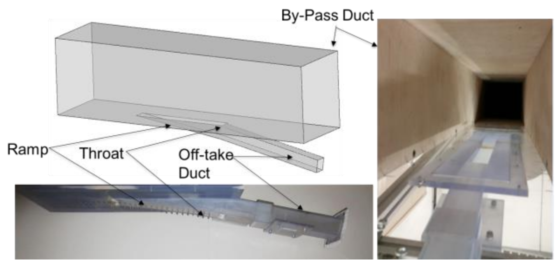

Figure 4: CFD Model and Off-take Test Rig

DATUM OFF-TAKE ANALYSIS

Figure 5 plots the RPR for the datum off-take, with an aspect ratio of 1, for varying velocity ratios from both the experimental and CFD data. At low VR the RPR is poor. This is due to the high off-take diffusion in conjunction with the fact that the majority of the captured flow comprises of low energy boundary layer flow. The flow is unable to overcome the adverse pressure gradient which causes thickening of the boundary layer along the ramp wall and eventually results in flow separation near the off-take throat. As the VR increases the RPR gradually increases as the captured streamtube area grows and comprises of a smaller portion of low quality boundary layer flow. However, as the VR increases further the RPR begins to reduce. Loss is increased initially due to the higher velocity and skin friction, but as the VR increases further the approach angle of the capture streamtube (see Figure 6b) generates a significant spillage drag in the off-take as the flow separates from the splitter leading edge. It must be noted that a similar phenomenon will cause spillage drag in the bypass at low VR (see Figure 6a). However, this has not been quantified in the current study.

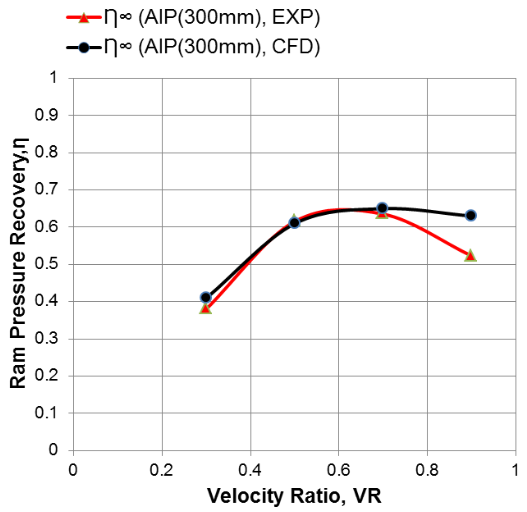

Figure 5: Experimental and CFD RPR (AS=1)

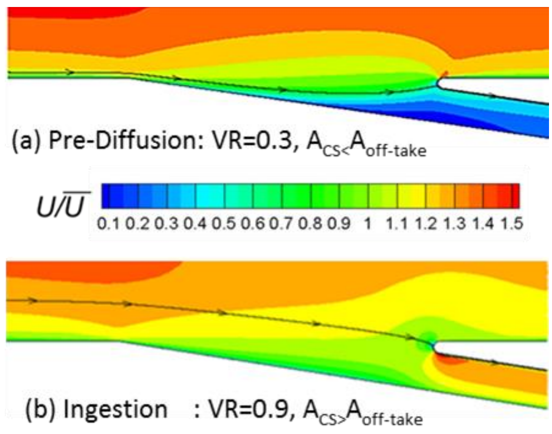

Figure 6: CFD Axial Velocity Contours - Effect of VR on Pre-diffusion and Incidence

Figure 7 is a plot (from the CFD) of the flow captured by the off-take, traced upstream of the inlet. It is interesting to compare the area of the captured flow to give a true indication of the level of diffusion undertaken by the off-take flow. For example, at a VR of 0.3 the captured streamtube is approximately 56% of the off-take width and 34% of the off-take height. Consequently the effective area ratio is 3.5. The flow must diffuse in both directions but more significantly in the vertical direction resulting in an increase in vertical non-uniformity (discussed later). At a higher VR of 0.9 the effective area ratio is just 1.2. The capture streamtube width is now broadly equal to the off-take width but the height is only 60% of the off-take. Diffusion, therefore, really only occurs in the vertical direction.

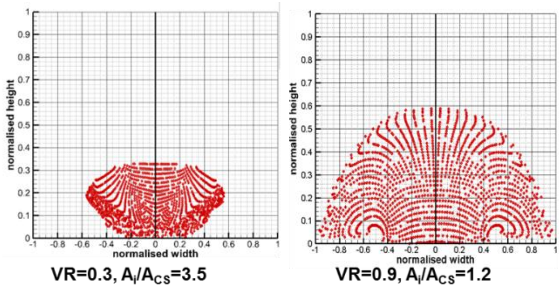

Normalised height = $h_{cs}/d_{off\text{-}take}$;

Normalised width = $w_{cs}/w_{off\text{-}take}$.

Figure 7: Effect of VR on Capture Streamtube Area and Diffusion

Understanding the 'true' diffusion is important. The RPR plotted in Figure 5 is computed based on using values from an inlet plane of area equal to the off-take throat (i.e. the traditional method). However, as seen in Figure 7 the captured stream tube represents only a portion of this. Furthermore it varies in size with VR and as a result different amounts of the inlet boundary layer are captured. With this in mind the RPR can be computed using values from the captured streamtube inlet. This analysis is limited to the CFD data and is plotted in Figure 8. The 'η_{cs}' is the RPR of the streamtube and is more representative of a true system performance.

Figure 9 plots normalised velocity contours (both experimental and CFD) at a plane 300mm downstream of the off-take throat. Note that due to the physical size of the five-hole probe used in the experiment it was not possible to measure right to the wall. However, the measured contoured and total pressure measurements agree reasonably well with the CFD.

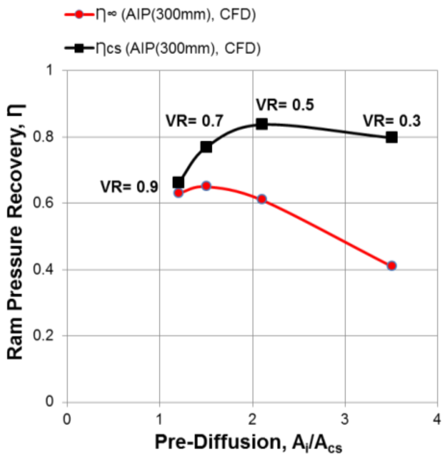

Figure 8: Effect of RPR with Respect to Capture Streamtube Diffusion (A_i/A_{cs}).

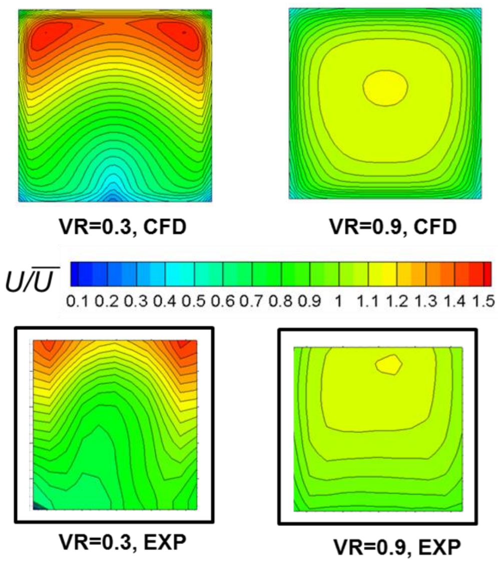

Figure 9: Normalised Axial Velocity (AIP 300mm) by Experiment and CFD, AS=1

It is evident that the uniformity at high VR is generally better than at low VR. In line with the previous arguments the higher vertical diffusion leads to poor uniformity in the vertical direction. The respective uniformity indexes are plotted in Figure 10. The vertical uniformity of flow increases with increased in VR while the horizontal uniformity decreases. Note that a single global parameter hides the directional differences in uniformity.

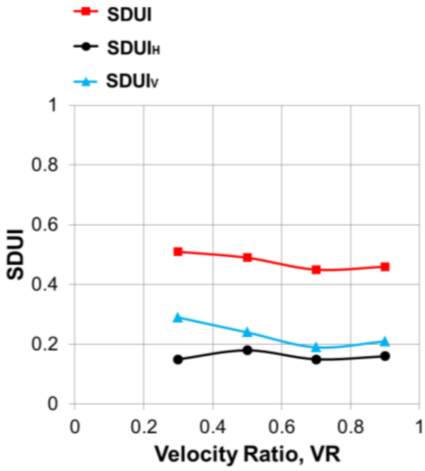

Figure 10: Datum Off-Take Uniformity

EFFECT OF INLET BOUNDARY LAYER

It has been shown that for a given inlet profile the performance of a flush off-take is a function of the VR. It then follows that the performance will also then be affected by the inlet boundary layer thickness. In fact this is one of the main disadvantages of a flush off-take in that it must ingest the poor quality upstream boundary layer. To further investigate the inflow boundary layer three profiles were employed in the CFD model of the flush off-take with an aspect ratio of 1. Shown in Figure 11 these included a naturally developed profile with δ/d = 1.5, a profile generated by a 10mm upstream trip and a profile scaled from an actual bypass duct profile downstream of the fan OGV.

Figure 12 shows that the area of the captured streamtube increases with the boundary layer thickness. The fact that the mean velocity at inlet relative to the captured streamtube is reduced means that the diffusion the streamtube undergoes is also reduced. Hence, for a VR of 0.3, the effective area ratio of the captured streamtube reduces from 3.5 to 2.5. The effect of this on the capture streamtube area ratio and RPR for varying VR is shown in Figure 13.

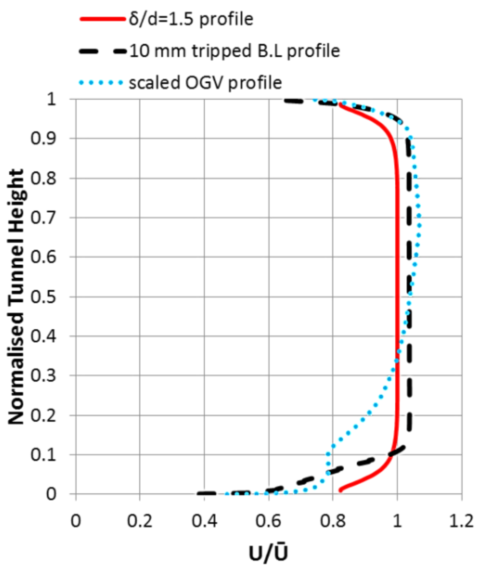

Figure 11: Inlet Boundary Layer Profiles

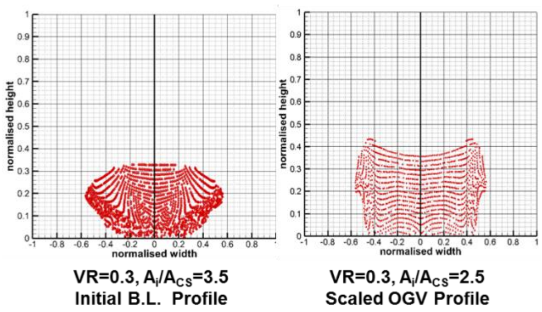

Figure 12: Effect of Inlet Boundary Layer Thickness on Capture Streamtube

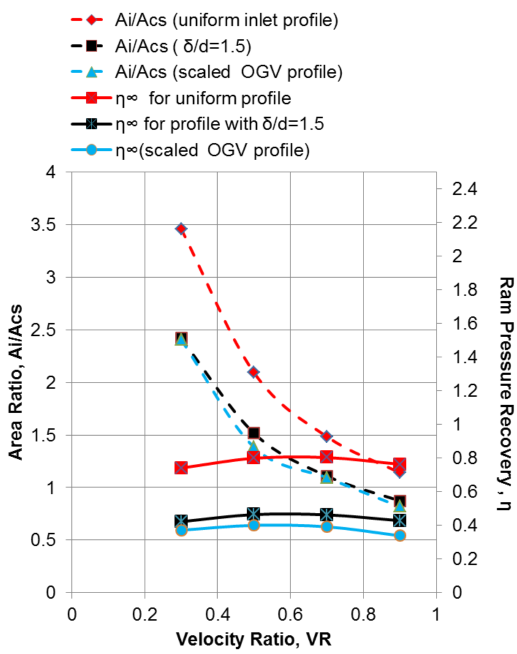

Figure 13: Effect of Inlet Boundary Layer Thickness on Area Ratio and RPR

Figure 14 shows the effect of inlet boundary layer thickness on the flow uniformity 300mm downstream of the off-take. In the case of the scaled OGV profile approximately 5% of RPR was lost compared to the uniform inflow profile. However, uniformity improved by 4% with increase in boundary layer thickness at low VR.

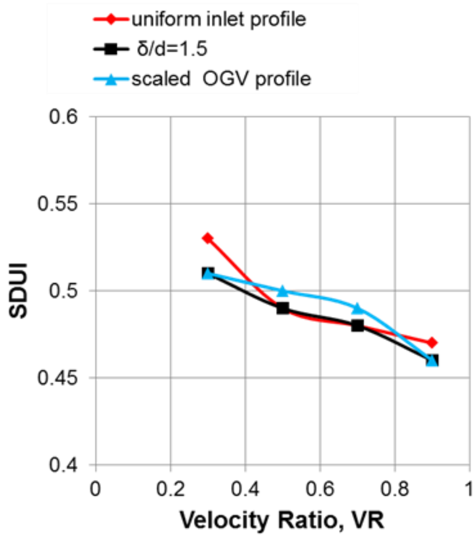

Figure 14: Effect of Inlet Boundary Layer Thickness on Exit Uniformity

EFFECT OF RAMP ANGLE (α)

The inclination or ramp angle of an off-take behaves in a manner similar to that of an asymmetric diffuser. The static pressure distribution for different ramp angles revealed that in all the cases of VR the flow undergoes a local acceleration due to a sudden change in the flow angle at the leading edge of the ramp (Figure 15). The pressure gradient at the lip does not affect the captured flow approximately up to 40% of the ramp planform length. As argued by Mossman and Randall [6] a higher angle means increased local diffusion, an adverse pressure gradient and increased boundary layer growth. If the ramp angle is excessive the flow will separate. Consequently, studies by Dennard [3] showed that an increase in ramp angle will decrease the RPR.

As shown in Figure 16 it is common practice that the ramp extends to the off-take throat. Thus there is a trade-off between ramp angle, off-take depth and system length.

For example for a fixed off-take depth a shallower angle may offset local diffusion and boundary layer growth but will result in a long off-take system.

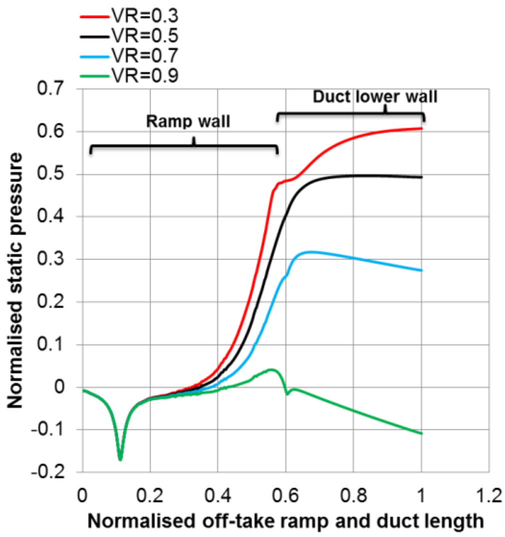

Normalised static pressure = p_{local}/p_{∞}

Normalised length = L/Total system length

Figure 15: Static Pressure Distribution on Off-Take Wall (7˚ ramp, δ/d=1.5)

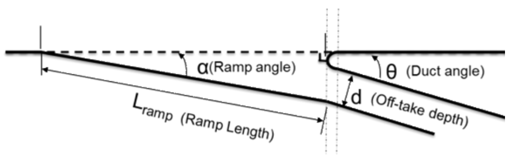

Figure 16: Ramp Angle Geometry

To examine the effect of ramp angle three cases (7˚, 10˚ and 15˚) were modeled numerically. Figure 17 shows axial velocity contours 300mm downstream of the off-take in conjunction with plots of the streamlines as they enter the off-take. At higher VR the increased incidence (see Figure 6) causes spillage into the off-take which generates vortices in the upper corners of the duct. This is made significantly worse by the higher ramp angles. As a result the peak velocity increases and shifts towards the lower walls. The RPR does not seem greatly affected (Figure 18) for an increase in ramp angle from 7° to 10°. However, with a ramp angle of 15° there is a degradation in RPR across all VRs of the flow seen in Figure 17. There is no real change in the global flow uniformity. There is a small, but on the whole negigible, degradation in horizontal and vertical uniformity with increased ramp angle (see Figure 19).

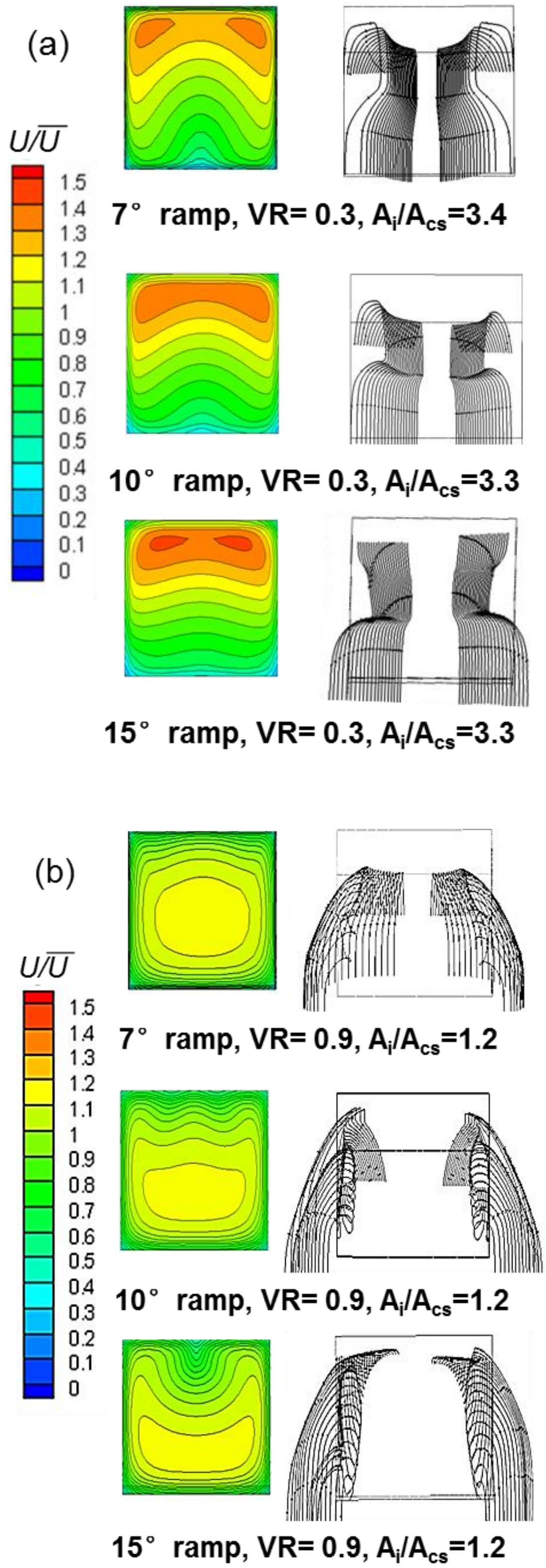

Figure 17 Normalised Axial Velocities (AIP 300mm) for Ramp Angles of 7˚, 10˚ and 15˚

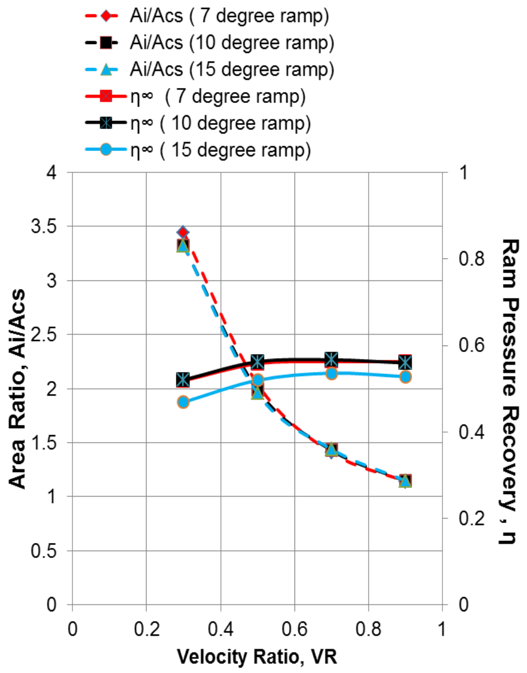

Figure 18: Effect of Ramp Angle on Area Ratio and RPR

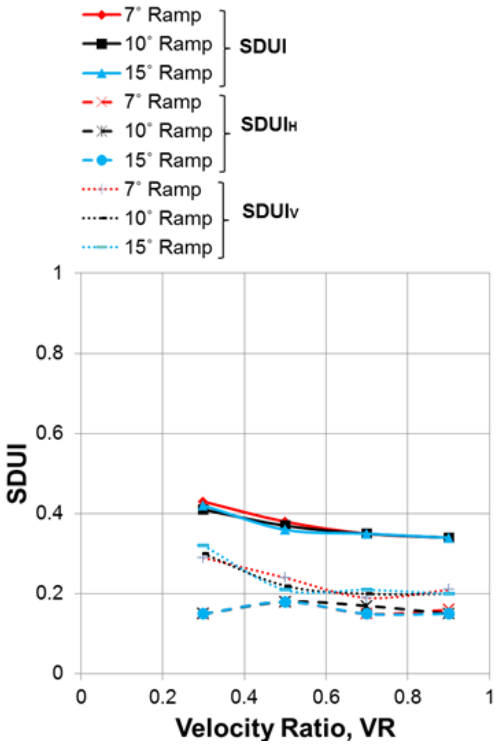

Figure 19: Effect of Ramp Angle on Uniformity

EFFECT OF WIDTH TO DEPTH RATIO (w/d) or ASPECT RATIO (AS)

With reference to Figures 15 and 20 the parameters that define the system geometry are interconnected. It is not possible to separate the effects of ramp length and width-to-depth (aspect) ratio [5]. For a given off-take throat area and ramp angle any changes in the ramp length will change the off-take height and hence the aspect ratio (Figure 20).

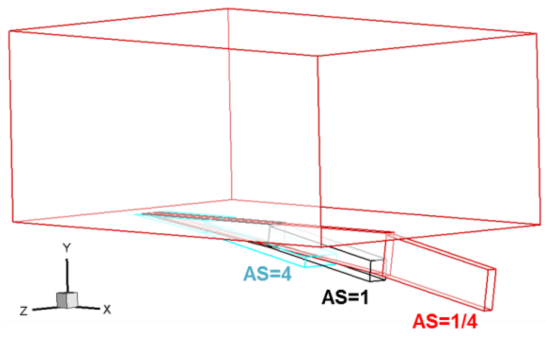

Figure 20: Influence of Off-take Aspect Ratio on System Length

There is conflicting data on the effect of aspect ratio. ESDU03006 [7] suggests that at high ramp angles changes of aspect ratio have a negligible effect on RPR and that a ratio of 4 (greater width) achieves a higher RPR at low VR. Experimental data from Reynolds and Reeder [8] suggests that a lower aspect ratio (greater height) is more favourable in terms of RPR. However, there are no conclusions on flow uniformity. To better understand the effects CFD models were created for off-takes with a 7° ramp, a 10° duct angle and aspect ratios of ¼ (narrow) and 4 (wide). The latter was also examined experimentally. Figure 21(a) presents axial velocity contours 300mm downstream of the off-take. For the AS of 4 there is good agreement between the predicted and measured contours. Clearly the uniformity is much worse at lower VR.

Examination of the captured stream tube (Figure 22) shows that changes in AS alter the shape of the captured flow. This is important for several reasons. Firstly, it subtly alters the area ratio of the captured streamtube (see Figure 23). Secondly, it also affects the direction that flow must expand/diffuse in, which has implications on the uniformity (see Figure 21(b)).

At low VR the AS 4 off-take performs better in terms of RPR (Figure 23), whereas the opposite is true at high VR when the AS of ¼ performs better. In general, poor RPR at low VR is due to high diffusion in the vertical direction so clearly a wider off-take with a higher AS will be beneficial. Similarly reduction of RPR at high VR is generally caused by spillage drag. A tall, narrow off-take is better in this case as the spillage flow is limited to a smaller outboard region of the off-take. Figure 24 plots the uniformity index for different AS off-takes. There is a significant reduction in global uniformity with the decrease in AS. The change in vertical uniformity between the AS 1 and AS 4 off-takes were negligible. The AS ¼ off-take suffered a 70% loss in vertical uniformity compared to other cases, but with an increase in VR the vertical uniformity of AS ¼ off-take improved rapidly, suggesting that the AS ¼ off-take performs better at higher VR. The horizontal uniformity shows an overall degradation for all VRs with a decrease in AS from 4 to ¼.

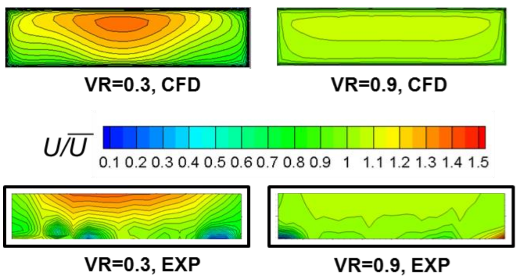

(a) Aspect Ratio 4

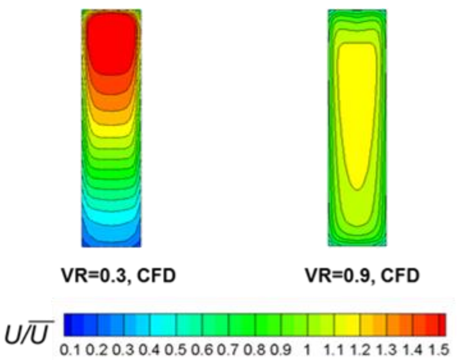

(b) Aspect Ratio ¼

Figure 21: Normalised Axial Velocity (AIP 300mm

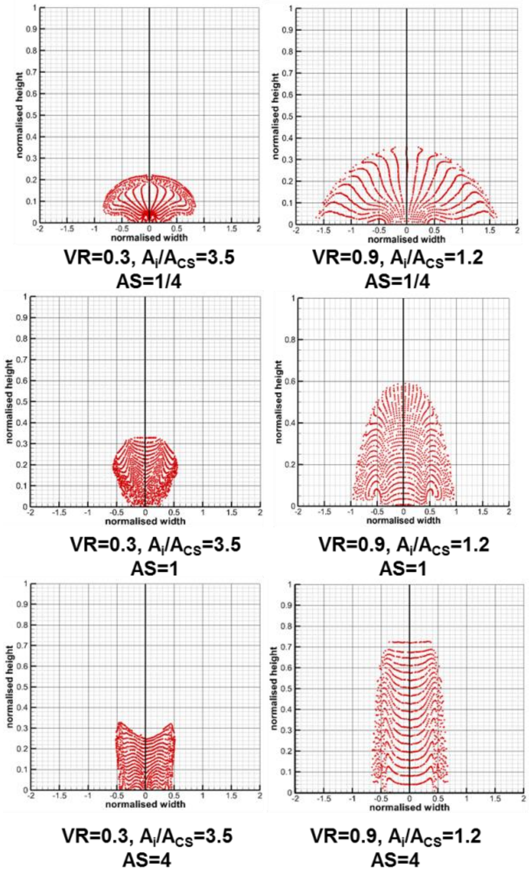

Figure 22: Effect of Aspect Ratio on the Captured Streamtube

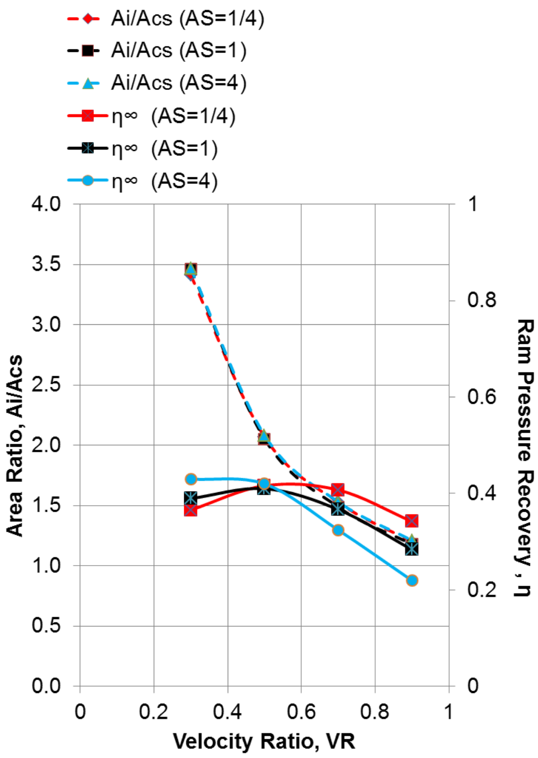

Figure 23: Effect of Aspect Ratio on Area Ratio and RPR

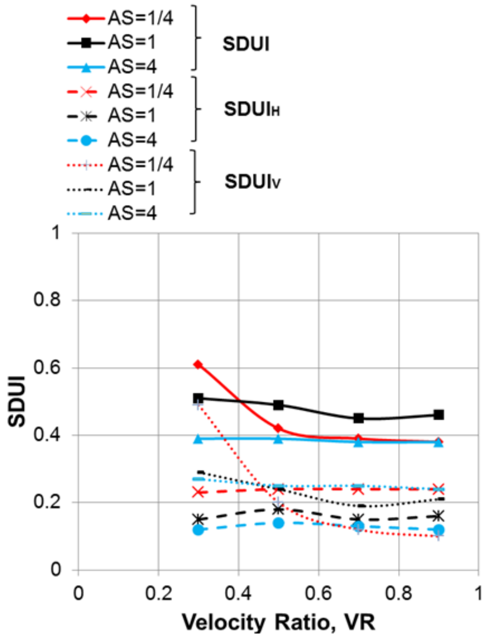

Figure 24: Effect of Aspect Ratio on Uniformity

EFFECT OF WALL DIVERGENCE

The effects of parallel and divergent wall off-takes have been studied by several authors. For example, Mossman [9] and Taylor [10] both showed that a divergent off-take can have a better RPR than a parallel wall off-take. A study by Delany [11] showed that the stream lines from a divergent flow are predominantly three dimensional with vortex pairs rammed into the off-take.

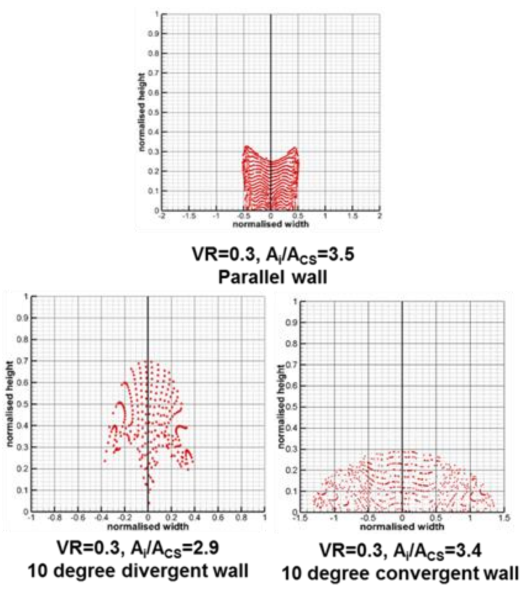

Figure 25: Effect of Wall Divergence on Captured Streamtube

Sacks et al. [12] stated that both divergent and convergent off-takes had similar flow behavior but in the case of convergent wall the vortex pair curved away from inlet and thus has less influence over off-take RPR.

To further investigate this and assess the effect on uniformity a 10˚ divergent and a 10˚ convergent wall off-takes were computationally modelled. It was found that the divergence angle has a significant effect on the captured streamtube profile. For example, Figure 25 shows the captured area at a VR of 0.3. It is worth noting that the 10˚ convergent off-take and AS of ¼ followed a similar trend in capture streamtube profile, i.e. the capture stream area grew along its width, capturing large portions of the boundary layer which then resulted in a low RPR.

Figure 25 shows that both the divergent and convergent walls cause an increase in the area of the captured streamtube relative to a parallel wall. In turn this reduces the area ratio of the streamtube. There was an increase in the height of the captured flow for divergent walls and a notable move away from the wall. This is significant as it means that the relative amount of boundary layer flow captured was reduced and the RPR improved as shown in Figure 26. Conversely, there was an increase in width of the captured streamtube for the convergent walls. This means a higher proportion of boundary layer is ingested and the RPR reduces.

Figure 27 suggests that there is a noticeable change in the global and horizontal flow uniformity. Although the convergent off-take shows better horizontal uniformity than the divergent wall, but with a 22% penalty in RPR, the parallel wall off-take has the highest level of global, vertical and horizontal uniformity than the diverged and converged wall.

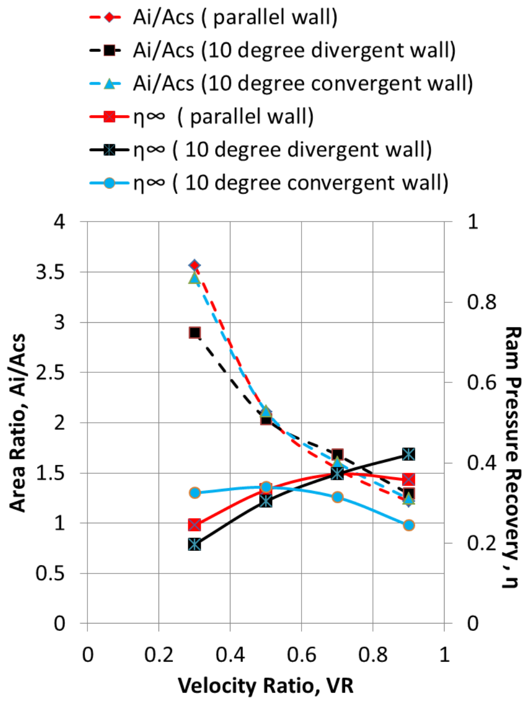

Figure 26: Effect of Wall Divergence on Area Ratio and RPR

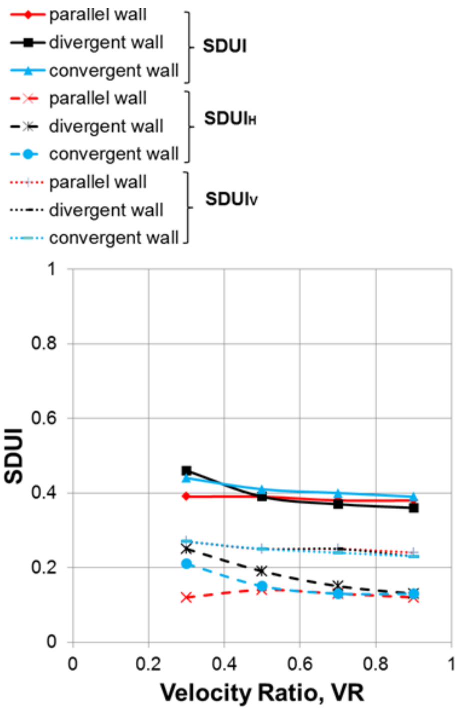

Figure 27: Effect of Wall Divergence on Uniformity

CONCLUSIONS

The RPR analysed and measured in the current analysis followed similar trends to that reported in several other works. The overall uniformity always decreased with an increase in pre-diffusion. The changes in VR and geometric parameters in an off-take had less influence on the horizontal uniformity.

The amount of pre-diffusion is relatively reduced for a given VR with increase in boundary layer thickness of the inflow profile. Although a thick boundary layer inflow reduces the overall RPR, it certainly improves the uniformity of the flow during pre-diffusion.

A low ramp angle is suitable for its high yield of RPR but a trade-off is necessary between reduction in ramp length and reduction in ramp angle. However, the uniformity was less influenced by changes in ramp angle.

The off-take aspect (w/d) ratio can be used as an effective tool for reducing the overall length of the off-take. In a flush off-take a major proportion of pre-diffusion occurs along the vertical direction and it was understood that the divergence of streamlines has to be kept to a minimum to improve the vertical uniformity. This can be done by either increasing the area of the capture streamtube or by keeping the off-take height to its minimum. A high aspect ratio off-take (reduced height and increased width) is therefore recommended for better uniformity and RPR.

Both the performance and uniformity of a divergent wall off-take is poorer at high pre-diffusion levels compared to the convergent and parallel wall off-takes. The convergent off-take showed a 10% improvement in RPR with a decrement of 13% in global uniformity compared to the parallel wall off-take.

It is possible to use the current off-take design investigation and optimise the design parameters in order to have an effective trade-off between RPR and uniformity of the flow exiting an off-take.

REFERENCES

1. Wilfert, G., Sieber, J., Rolt, A., Baker, N., Touyeras, A., and Salvatore, C., 2007, "New Environmental Friendly Aero Engine Core Concepts", ISABE-2007-1120, 18th ISABE Conference, Beijing.
2. Walker, A. D. and Guo, L., 2015, "Impact of a Cooled Cooling Air Installation on the External Aerodynamics of a Gas Turbine Combustion System", ASME Paper No. GT2015-43183.
3. Dennard, J. S., 1957, "A Transonic Investigation of the Mass-Flow and Pressure Recovery Characteristics of Several Types of Auxiliary Air Inlets", NACA RM L57B07.
4. Bissinger, N. C. and Breuer, T., 2010, "Basic Principles – Gas Turbine Compatibility – Intake Aerodynamic Aspects", Encyclopedia of Aerospace Engineering, John Wiley & Sons, Ltd.
5. Devine, R. J., Watterson, J. K. and Cooper, R. K., 2004, "Performance Improvement of Flush, Parallel Walled Auxiliary Intakes By Means Of Vortex Generators", Proceedings of the 24th International Congress for Aeronautical Sciences.
6. Mossman, E. A. and Randall, L. M., 1948, "An Experimental Investigation of the Design Variables for NACA Submerged Duct Entrances", NACA RM A7I30.
7. ESDU03006, 2003, "Subsonic Drag and Pressure Recovery of Rectangular Planform Flush Auxiliary Inlets with Ducts at Angles up to 90 Degrees".
8. Reynolds, T. and Reeder, M. F., 2009, "Variation of Flow Control Configurations to Improve Submerged Inlet Uniformity", AIAA 2009-1259 47th AIAA Aerospace Sciences Meeting.
9. Mossman, E. A., 1949, "A Comparison of Two Submerged Inlets at Subsonic and Transonic Speeds", NACA RM A9F16.
10. Taylor, R. A., 1952, "Some Effects of Side-Wall Modifications on the Drag and Pressure Recovery of an NACA Submerged Inlet at Transonic Speeds", NACA RM A51LO3a.
11. Delany, N. K., 1948, "An Investigation of Submerged Air Inlets on a 1/4-Scale Model of a Typical Fighter-Type Airplane", NACA RM A8A20.
12. Sacks, A. H. and Spreiter, J. R., 1951, "Theoretical investigation of submerged inlets at low speeds", NACA Technical Note 2323.